Biophysical Journal Volume 107 August 2014 654–661

Article

# UNC-45B Chaperone: The Role of its Domains in the Interaction with the Myosin Motor Domain

Paul J. Bujalowski,[1,2] Paul Nicholls,[1,2] and Andres F. Oberhauser[1,3,*]
[1]Department of Neuroscience and Cell Biology, [2]Department of Biochemistry Molecular Biology, and [3]Sealy Center for Structural Biology and Molecular Biophysics, University of Texas Medical Branch, Galveston, Texas

ABSTRACT The proper folding of many proteins can only be achieved by interaction with molecular chaperones. The molecular chaperone UNC-45B is required for the folding of striated muscle myosin II. However, the precise mechanism by which it contributes to proper folding of the myosin head remains unclear. UNC-45B contains three domains: an N-terminal TPR domain known to bind Hsp90, a Central domain of unknown function, and a C-terminal UCS domain known to interact with the myosin head. Here we used fluorescence titrations methods, dynamic light scattering, and single-molecule atomic force microscopy (AFM) unfolding/refolding techniques to study the interactions of the UCS and Central domains with the myosin motor domain. We found that both the UCS and the Central domains bind to the myosin motor domain. Our data show that the domains bind to distinct subsites on the myosin head, suggesting distinct roles in forming the myosin–UNC-45B complex. To determine the chaperone activity of the UCS and Central domains, we used two different methods: 1), prevention of misfolding using single-molecule AFM, and 2), prevention of aggregation using dynamic light scattering. Using the first method, we found that the UCS domain is sufficient to prevent misfolding of a titin mechanical reporter. Application of the second method showed that the UCS domain but not the Central domain prevents the thermal aggregation of the myosin motor domain. We conclude that while both the UCS and the Central domains bind the myosin head with high affinity, only the UCS domain displays chaperone activity.

## INTRODUCTION

The specific three-dimensional structure is one of the major determinants of protein function (1). In some protein systems, complex structures can only be formed by interacting with specific molecular chaperones (2). Chaperones are specific protein factors, which prevent aggregation, e.g., DnaJ, Hsp33, or promote efficient folding, e.g., GroEL/GroES (3–6). In the case of muscle development, one of the major problems is the elucidation of the coordinated action of several chaperones that are required for the formation of myosin thick filaments. In these processes, the formation of the native structure of myosin is achieved only through intricate interactions with molecular chaperones, including UNC-45B, Hsp90, and Hsp70 (7–15). Myosins are a diverse superfamily of protein motors with at least 24 distinct classes (16). The general structure of the myosin molecule, including the type-II myosin involved in muscle structure, includes the myosin head (motor domain), the neck, and the tail domains (17). The motor domain harbors the sites for the actin binding and the enzymatic activities. Although the tail domain can fold spontaneously, the motor domain requires the action of several molecular chaperones to fold into a fully functional structure head (10–12,18,19). The myosin-specific chaperone UNC-45B, a founding member of the UCS (UNC-45/Cro1/She4p) family of proteins (20,21), is essential for proper folding and assembly of myosin into muscle thick filaments (22). All metazoan genomes analyzed thus far encode an UNC-45 ortholog. In vertebrates, there are two *unc-45* genes, a general cell isoform UNC-45A, and a muscle-specific isoform, UNC-45B (23).

UNC-45B is composed of three domains: An amino-terminal tetratricopeptide repeat (TPR) domain known to interact with the ubiquitous molecular chaperone heat shock protein 90 (Hsp90) (10), a 390-residue Central of unknown function, and a 430-residue C-terminal UCS domain that has been identified to partially rescue the uncoordinated phenotype in *Caenorhabditis elegans* (24) (Fig. 1). Genetic and biochemical studies have highlighted the importance of UCS-domain-containing proteins for proper myosin function. UNC-45B prevents aggregation of thermally denatured myosin subfragment 1 (myosin S1, comprised almost exclusively of the motor domain; we use S1 and motor domain interchangeably throughout the text) (10,25) and prevents misfolding of mechanically unfolded myosin S1 (26).

The x-ray crystal structures of the yeast protein She4p homolog, *Drosophila*, and *Caenorhabditis elegans* UNC-45, have been determined (9,27,28). Despite recent advances on the structural characterization of these chaperones, the molecular mechanisms by which they interact with the myosin motor domain remain poorly understood.

*Submitted April 8, 2014, and accepted for publication May 29, 2014.*
*Correspondence: afoberha@utmb.edu
Editor: Enrique De La Cruz.

0006-3495/14/08/0654/8 $2.00
http://dx.doi.org/10.1016/j.bpj.2014.05.045

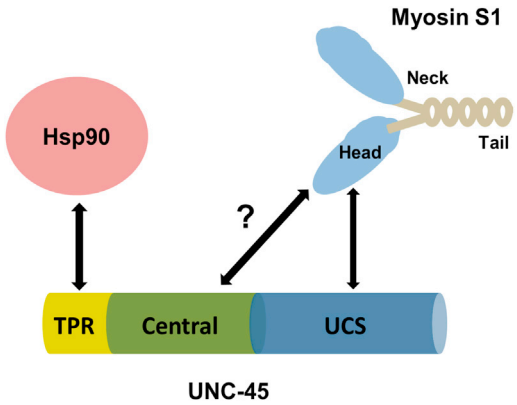


FIGURE 1 Myosin II is composed of a motor domain and an extended rodlike coiled-coil domain. UNC-45B is made of $\alpha$-helical tandem repeat motifs with three distinct domains: an 100-amino-acid amino-terminal TPR domain that interacts with Hsp90, a 389-amino-acid Central domain of unknown function, and a 430-amino-acid UCS domain that associates with the myosin motor domain. To see this figure in color, go online.

Furthermore, even less is known about the nature of the interactions between myosin and the UNC-45B domains. Although it has been suggested that direct interactions between myosin and the UCS domain occur (24), the energetics of the process have not been quantified. The role of the Central domain in the myosin/UNC-45B interactions is unknown.

In our approach, we applied a combination of complementary experimental approaches (fluorescence titration of BADAN-labeled S1, dynamic light scattering, and single-molecule AFM technique) to quantitatively analyze the interactions of UNC-45B domains with the myosin motor domain. We discovered that the UCS domain and the Central domain bind to different subsites on the myosin head, suggesting distinct roles in forming the myosin−UNC-45B complex. Our data indicate that the UCS domain alone is sufficient to prevent myosin misfolding and aggregation. Hence, the UCS domain likely plays a critical role in the biogenesis and proper folding of the myosin motor domain.

## MATERIALS AND METHODS

### Proteins

#### *Myosin*

Myosin was purified from rabbit skeletal muscle using established protocol (29). Myosin subfragment 1 (S1, comprised almost exclusively of the motor domain; we use "S1" and "motor domain" interchangeably throughout the text) was obtained by chymotryptic digestion of myosin as described in Weeds and Pope (30) and Mornet et al. (31). The purity of the myosin motor domain was confirmed by sodium dodecyl sulfate-polyacrylamide gel electrophoresis (SDS-PAGE) (Fig. 2 *A*).

#### *UNC-45B constructs*

The selection of domain boundaries for the UCS domain (500–931 amino acids) and the Central domain (100–499 amino acids) were based on the human UNC-45B sequence (Accession No.: Q8IWX7.1) and crystal structure (9,28) (see Fig. S1 in the Supporting Material). UNC-45B is highly conserved among mammals. The alignment between human and mouse UNC-45B showed 95% identity and 98% similarity and 99% identity and 99% similarity between the human and mouse UCS domain. Synthetic cDNA (GenScript) for the constructs were subcloned into a pProEx vector (Life Technologies, Carlsbad, CA) for UNC-45B or pET28a vector (EMD Millipore, Billerica, MA) for the UCS and Central domains; the N-terminus had a hexahistidine ($His_6$) tag. Protein expression in BL21 cells (Life Technologies) was induced by addition of 1 mM IPTG and shaking at 16°C overnight. The cells were resuspended in PBS (phosphate-buffered saline,

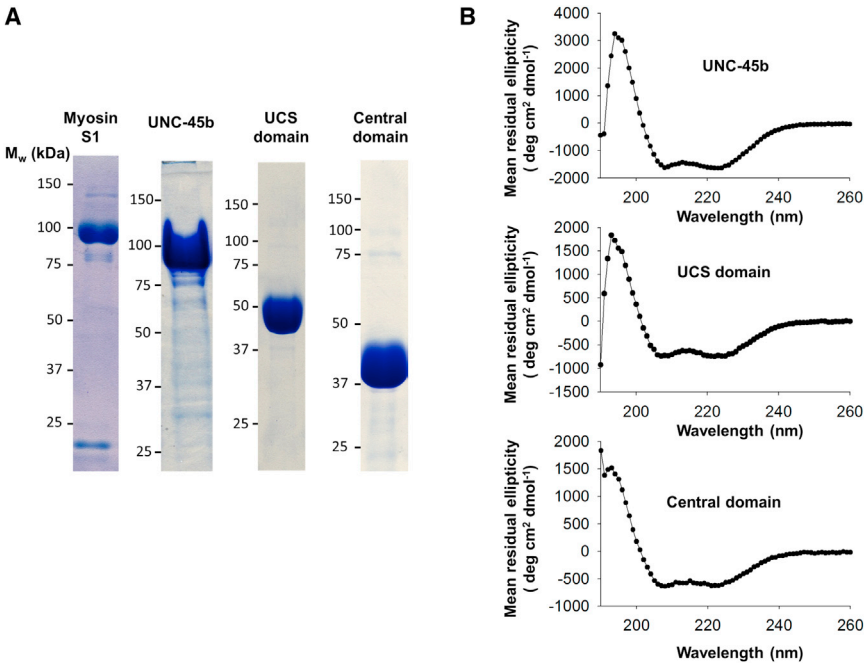


FIGURE 2 Characterization of the full-length UNC-45B and its UCS and Central domains. (*A*) SDS-PAGE gels of the purified proteins: Myosin S1, UNC-45B, UCS domain, and Central domain. (*B*) Far-UV circular-dichroism spectroscopy for a full-length UNC-45B (*top*), UCS domain (*center*), and Central domain (*bottom*). All three of them exhibit typical $\alpha$-helix secondary structure with minima at 209 and 222 nm (58, 69, and 69% for full-length UNC-45B, UCS, and Central domains, respectively). To see this figure in color, go online.

10 mM sodium phosphate buffer, pH 7.4, 150 mM NaCl), and sonicated on ice in the presence of a protease inhibitor cocktail (1 mM phenylmethylsulfonyl fluoride and 1 g/mL of trypsin inhibitor, chymostatin, pepstatin, leupeptin, *N*-benzoyl-L-arginine ethyl ester, and *p*-toluidinyl-L-arginine methyl ester). The proteins were affinity-purified over a HisTrap column (GE Healthcare, Piscataway, NJ), eluting with a gradient from 20 to 500 mM imidazole over 20 column volumes. The $His_6$-tags were cleaved using thrombin (UCS and Central domain) or TEV protease (UNC-45B). The purity of the proteins was confirmed by SDS-PAGE and was >95% (Fig. 2 *A*). Full-length UNC-45B has a similar molecular mass to myosin subfragment 1 (S1) and runs at ~100 kDa whereas the UCS and Central domains run slightly below 50 kDa (molecular masses are 46 and 44 kDa, respectively).

### *Chimeric I27-myosin S1 construct (I27-S1 protein)*

We used our previously published protocol to chemically couple an octameric I27 polyprotein to a specific site within the myosin motor domain of myosin S1 (26). The polyprotein harbored an N-terminal cysteine residue and a C-terminal $His_6$-tag. Coupling to the S1 was achieved via the reactive cysteines (SH1/SH2) within the motor domain. The cross-linking adduct was isolated by size-exclusion chromatograpy on a Sephacryl S-300 column (GE Healthcare). This protein chimera was found to be properly folded because it binds actin filaments in an ATP-dependent manner and can support actin filament gliding (see Fig. S2).

## Circular dichroism

The far ultraviolet (UV) circular-dichroism measurements were performed on a model No. J-815 spectrometer (JASCO, Oklahoma City, OK). The protein concentration was 1 $\mu$M in 30 mM TRIS pH 7.4, 100 mM KCl, 1 mM $MgCl_2$, and 1 mM TCEP buffer. A 0.2-cm path-length cuvette was used. The data reported in Fig. 2 *B* corresponds to the average of three scans obtained at a scan rate of 50 nm/min in the range of 190–260 nm. The software program K2D3 (http://www.ogic.ca/projects/k2d3/) was used to estimate secondary protein structure content.

## Fluorescence measurements

The environmentally sensitive fluorophore BADAN attached to myosin S1 was used to study its interaction with full-length UNC-45B and its UCS and Central domains (26). The fluorescence titrations were done in the presence of 100 mM KCl, 1 mM $MgCl_2$, 30 mM TRIS pH 7.4, and 1 mM TCEP. Experiments were performed in a quartz cuvette (500 $\mu$L) into which the UNC-45B constructs (full-length UNC-45B, UCS domain, and Central domain) were added. Fluorescence emission of BADAN-S1 at 520 nm was measured after excitation at 387 nm relative to a control sample that contained buffer instead of UNC-45B constructs. Each point of the titration curve corresponds to an average of 20 measurements. Steady-state fluorescence titrations were performed using an ISS PC1 spectrofluorometer (ISS, Urbana, IL). To avoid possible artifacts due to the fluorescence anisotropy of the sample, polarizers were placed in excitation and emission channels and set at 90 and 55° (magic angle), respectively. Nonlinear least-square fits were done using the softwares KALEIDAGRAPH (Synergy Software, Reading, PA) and MATHEMATICA (Wolfram Research, Champaign, IL).

## Single-molecule atomic force microscopy

The mechanical properties of single I27-S1 protein chimeras were investigated using a home-built single-molecule AFM as previously described in the literature (26,32–36). The spring constant of each individual cantilever (MLCT or Olympus OBL, Veeco Metrology Group, Santa Barbara, CA) was determined experimentally by measuring the cantilever power spectrum and using the equipartition theorem (37). A small volume of the purified I27-S1 chimera (~1–5 $\mu$L, 10–100 $\mu$g/mL) was allowed to adsorb an Ni-NTA coated-glass coverslip (38) for ~10 min and then was rinsed with PBS pH 7.4. Proteins were picked up randomly by adsorption to the cantilever tip, which was pressed down onto the sample for 1–2 s at forces of several nanoNewtons and then stretched for several hundred nm. All experiments were performed at room temperature (~25°C) at a pulling speed of 0.5–0.7 nm/ms.

A two-pulse unfolding/refolding protocol was used to estimate the fraction of refolded domains (26,33,39). After the first stretch, a single I27-S1 protein chimera was allowed to relax for time intervals of ~10 s. In the second pulling, we counted the refolded domains. The number of the domains that refolded in the second pulling divided by the number of the unfolded domains in the first pulling gives the fraction of refolded I27 domains. In a typical experiment, after picking up a protein, the AFM tip was moved away from the surface (~30–50 nm) to prevent the tip picking up new proteins due to cantilever drift.

# RESULTS AND DISCUSSION

## Characterization of the full-length UNC-45B and its UCS and Central domains

In order to examine the structural integrity of the UNC-45B constructs, the overall secondary structure was determined using far-UV circular dichroism. We found that the secondary structure shows a predominantly $\alpha$-helical content (Fig. 2 *B*), which is consistent with the available crystal structure data showing that UNC-45B is composed almost entirely of $\alpha$-helical armadillo repeats (9,27,28).

## Tracking UCS domain binding to the myosin motor domain

We took advantage of the environmentally sensitive fluorophore BADAN attached to myosin S1 to monitor its interaction with the UNC-45B protein constructs (26). The BADAN fluorophore has been shown to react preferentially with the SH1 group (44), yielding fluorescently labeled myosin S1 (BADAN-S1) with a reporter fluorophore at a specific site (Cys-707) within the catalytic domain. We found that the UCS domain induced a decrease in BADAN fluorescence emission intensity with increasing UCS domain concentrations, indicating that the local environment of the fluorescent probe changes due to interaction of BADAN-S1 with the UCS domain (Fig. 3 *A*). This change could be the consequence of either direct binding near the catalytic site, or of allosteric changes in the motor domain upon binding at a distal site.

The simplest model that describes this titration curve is a binding system that assumes complex formation with a 1:1 stoichiometry of UCS and BADAN-S1, described by Eq. 1 (see Appendix in the Supporting Material for derivation of Eq. 1 and for Eqs. S9–S15),

$$\Delta F_{\mathrm{obs}} = \frac{F_{\mathrm{obs}}}{F_F[\mathrm{S1}]_T} = \frac{1}{1+K_1[\mathrm{UCS}]_F} + \Delta F_{\max}\left(\frac{K_1[\mathrm{UCS}]_F}{1+K_1[\mathrm{UCS}]_F}\right), \quad (1)$$

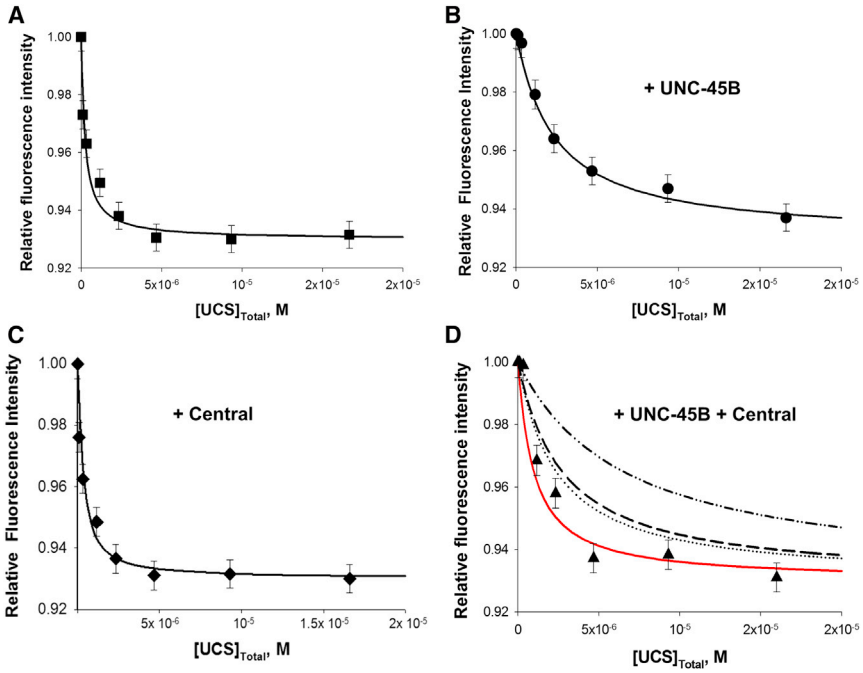


FIGURE 3 Tracking UNC-45B–myosin head interactions using an environmentally sensitive fluorescent probe. (*A*) BADAN-S1 fluorescence emission as a function of the total UCS domain concentration; (*solid line*) fit of Eq. 1 to the data assuming a complex formation with a 1:1 stoichiometry of UCS and BADAN-S1, yielding an apparent binding constant of $K_1 = 4.3 \times 10^6$ $M^{-1}$. The BADAN-S1 concentration was $2.5 \times 10^{-7}$ M. (*B*) Titration of BADAN-S1 ($2.5 \times 10^{-7}$ M) with the UCS domain in the presence of full-length UNC-45B ($3 \times 10^{-6}$ M). (*Solid line*) Best-fit of Eq. S9 in the Supporting Material to the data using $K_2 = 2.8 \times 10^6$ $M^{-1}$. (*C*) Titration of BADAN-S1 ($2.5 \times 10^{-7}$ M) with the UCS domain in the presence of the Central domain ($3 \times 10^{-6}$ M). Data show no competition between both domains. (*Solid line*) Best-fit to the data yielding $K_1 = 4.5 \times 10^6$ $M^{-1}$. (*D*) Titration of BADAN-S1 with the UCS domain in the presence of UNC-45B and Central domain. BADAN-S1 ($2.5 \times 10^{-7}$ M) fluorescence emission as a function of the total UCS domain concentration in the presence of full-length UNC-45B ($3 \times 10^{-6}$ M) and Central domain ($3 \times 10^{-6}$ M). (*Dotted black lines*) Analysis of the experimental data using a triple competition single-binding site model (see Eq. S14 in the Supporting Material); the binding constants for UCS, UNC-45B, $K_1$, and $K_2$, respectively, were from the experiments shown in panels *A* and *B*. (*Lines*) Different values for the association constant for the Central domain, $K_3$, ranging from $6 \times 10^6$ to $6 \times 10^3$. (*Solid red line*) Best-fit to a triple competition two-binding site model (see Eq. S15 in the Supporting Material) yielding a $K_3 = 6 \times 10^5$ $M^{-1}$. To see this figure in color, go online.

where $F_{obs}$ is the measured emission fluorescence, $K_1$ is the UCS association constant, $[UCS]_F$ is the free concentration of the UCS domain, *S1* is BADAN-S1, $F_F$ and $F_C$ are the molar fluorescence intensities of the free BADAN-S1 and the complex BADAN-S1-UCS, and $\Delta F_{max} = F_C/F_F$ is the maximum value of the observed relative fluorescence quenching. Because, under our experimental conditions the total $[UCS]_T >> [BADAN\text{-}S1]_T$, we can assume that $[UCS]_F \approx [UCS]_T$. The solid line in Fig. 3 *A* corresponds to a nonlinear least-squares fit of Eq. 1 to the experimental data, yielding an equilibrium association constant, $K_1 = (4.3 \pm 1.5) \times 10^6$ $M^{-1}$. The observed quenching of BADAN-S1 with the UCS domain (~7%) indicates the domain induces changes in the chemical environment around the fluorophore, likely increasing the solvent accessibility in the near proximity of BADAN and/or enhancing short-range interactions between the fluorophore and local molecular environments (45).

## UNC-45B and its UCS domain compete for a binding site on the myosin motor domain

We found that, under the same salt conditions (100 mM KCl, 1 mM $MgCl_2$, 30 mM TRIS pH 7.4), titrating BADAN-S1 with full-length UNC-45B interaction does not result in a change of the fluorophore emission intensity. Because the presence of the chaperone does not induce any change of fluorescence signal, we performed direct competition studies of the UCS domain binding to myosin in the presence of UNC-45B. The relative fluorescence intensity of the BADAN-S1, as a function of the UCS concentration, in the presence of $3 \times 10^{-6}$ M UNC-45B is shown in Fig. 3 *B* (*solid circles*). The curve is shifted toward higher fluorescence values than in the absence of UNC-45B, suggesting that they compete for the same binding site. The titration curve was analyzed using a macromolecular competition titration method (46–48) and Eq. S9 (see Appendix in the Supporting Material). This method provides a way to quantitatively examine binding of multiple protein ligands to any macromolecule with single or multiple binding sites (46–48). The line in Fig. 3 *B* corresponds to a nonlinear least-squares fit of Eq. S9 in the Supporting Material to the experimental data yielding a $K_2 = (2.8 \pm 0.8) \times 10^6$ $M^{-1}$. This value, obtained at 100 mM KCl, is similar to our previously reported affinity of the UNC-45B–myosin complex $(1.4 \pm 0.5) \times 10^6$ $M^{-1}$, determined using a lower salt concentration (30 mM KCl) buffer (26).

## The Central domain of UNC-45B binds to the myosin motor domain

Similar to the full-length UNC-45B, in our buffer conditions the isolated Central domain does not induce any change of the BADAN-labeled myosin fluorescence intensity (data not shown). Fig. 3 *C* shows an example of a fluorescence

titration experiment of BADAN-S1 with the UCS domain in the presence of the Central domain ($3 \times 10^{-6}$ M). The data indicate that the Central domain does not affect UCS–S1 interactions. This may result either from the lack of interactions between the Central domain and the myosin motor domain or from the lack of competition between the domains for myosin.

Because neither UNC-45B nor the Central domain induce any fluorescence change of the BADAN-S1, we carried out direct competition studies of the UCS binding to myosin in the presence of the UNC-45B chaperone and the Central domain. The fluorescence titration of BADAN-S1 with the UCS domain in the presence of full-length UNC-45B ($3 \times 10^{-6}$ M) and Central domain ($3 \times 10^{-6}$ M) is shown in Fig. 3 *D* (*black triangles*). Surprisingly, the presence of the Central domain shifts the titration curve to lower fluorescence values compared to UNC-45B alone, suggesting a complex type of interaction with the motor domain. We first consider a model where UNC-45B and its UCS and Central domains compete for the same binding site on the myosin head. The dotted black lines represent the predictions of a triple-competition single-binding site model (Fig. 3 *D*) as described by Eq. S13 (see the Supporting Material). Each dotted line corresponds to different values calculated using Eq. S13 in the Supporting Material using an association constant, $K_3$, ranging from $6 \times 10^6$ to $6 \times 10^3$ for the Central domain. It is clear that a single-binding site model is inadequate to describe the experimental data.

Next, we consider a model where UNC-45B binds to two binding sites on the myosin motor domain. The data was analyzed using a triple-competition two-binding model (see Eq. S15 in the Supporting Material). The solid red line corresponds to the best-fit of Eq. S15 in the Supporting Material to the experimental data, yielding an apparent association constant, $K_3$, of $(6.0 \pm 2.1) \times 10^5$ $M^{-1}$. This analysis indicates that the Central domain also binds to the myosin head but to a different subsite than the UCS domain. The data show that:

1. The UCS domain engages myosin with higher affinity than full-length UNC-45B, and
2. The Central domain binds with a weaker affinity than full-length UNC-45B and the UCS domain.

The fact that the UCS domain and the Central domain do not compete for the same binding site on myosin suggests they may have different functional roles in forming the myosin−UNC-45B complex.

## Allosteric interactions between the UCS and Central domains and myosin motor domain

Having determined the intrinsic affinities of the UCS and Central domains and the full-length UNC-45B chaperone for myosin S1 we estimated the energetics of these interactions. The binding of the full-length UNC-45B to S1 occurs with an affinity, $K_2$, of $2.8 \times 10^6$ $M^{-1}$, which gives a Gibbs free energy change of $\Delta G^0_{\text{UNC-45}} = 8.6$ kcal/mol. The Gibbs free energy change of the UCS and Central domains are tabulated below (Table 1). Therefore, free energy of UNC-45-S1 interaction is not a simple sum of the UCS and Central domain interactions with S1.The overall energetic contributions to the UNC-45-S1 complex can be described using the general approach proposed by Jencks (49),

$$\Delta G^0_{\text{UNC-45}} = \Delta G^0_{\text{UCS}} + \Delta G^0_{\text{Central}} + \Delta G^0_{\text{C}}, \qquad (2)$$

where $\Delta G^0_{\text{UCS}}$ and $\Delta G^0_{\text{Central}}$ are the intrinsic free energy changes accompanying binding of the isolated UCS and Central domains to the myosin S1, respectively. The single unknown in Eq. 2 is $\Delta G^0_{\text{C}}$, the additional intrinsic free energy change as a consequence of the allosteric conformational changes accompanying the UNC-45B–S1 complex formation. The estimated $\Delta G^0_{\text{C}}$ is −8 kcal/mol. Thus, these data indicate that the total free energy of UNC-45B–S1 interaction is not the simple sum of the energetic contributions of the UCS and Central domains; this suggests that the domains are not thermodynamically autonomous and allosteric interactions between them may play an important role in controlling the UNC-45B affinity for myosin.

## The UCS but not Central domain acts as a classical chaperone

Our BADAN fluorescence data clearly show that both UCS and Central domains interact with the myosin motor domain. To test the chaperone activity of the UCS and Central domains, we used two independent methods:

1. Prevention of S1 misfolding using single-molecule AFM (26), and
2. Prevention of heat-induced aggregation of S1 using dynamic light scattering (10,25).

In the first method, we used a titin molecular reporter approach to track chaperone-myosin interactions using AFM techniques (26). By chemically coupling a titin I27

**TABLE 1 Estimated equilibrium association constants and changes in Gibbs free energy of full-length UNC-45B and its UCS and Central domains for myosin S1**

| Protein | Full-length UNC-45B | UCS domain | Central domain |
|---|---|---|---|
| Association constant ($M^{-1}$) | $K_2 = (2.8 \pm 0.8) \times 10^6$ | $K_1 = (4.3 \pm 1.5) \times 10^6$ | $K_3 = (6.0 \pm 2.1) \times 10^5$ |
| $\Delta G^0$ (kcal/mol) | 8.6 | 8.5 | 7.7 |

polyprotein to the motor domain of myosin, we introduced a molecular reporter, providing a specific attachment point and a well-characterized mechanical fingerprint in single-molecule AFM experiments (33,50). This approach enabled us to study the folding/misfolding behavior of the motor domain and directly observe the effect of the chaperone UNC-45B (26). We found that the motor domain in the I27-S1 protein chimera is fully functional because it binds actin filaments in an ATP-dependent manner (not shown), and most importantly, is able to support actin-filament gliding (see Fig. S2). We subjected single titin I27-derivatized S1 molecules (Fig. 4 *A*) to repeated mechanical stretching in the AFM (Fig. 4 *B*), separated by pause intervals of 10 s at zero force (see Fig. 4 *B*, *inset*). I27 polyproteins unfold with a characteristic fingerprint (unfolding forces of ~200 pN and increases in contour length of ~30 nm) and readily refold through many repetitions without any signs of fatigue (33). However, when chemically linked to the myosin S1, the characteristic I27 sawtooth pattern is apparent only in the initial unfolding trace and absent in the second and third traces, indicating that the unfolded motor domain interferes with refolding of the otherwise robust I27 modules, presumably by recruiting them into a misfolded state (26) (Fig. 4 *B*, *left panel*). In the presence of 1 $\mu$M UCS (Fig. 4 *B*, *right panel*), full recovery of folded I27 domains is observed. Control experiments show that the UCS domain does not affect the refolding efficiency of the I27 polyprotein alone. Similar results were obtained when using full-length UNC-45B (Fig. 4 *C*). In contrast, we found that the Central domain does not prevent misfolding of the titin domains in the I27–S1 protein chimera (Fig. 4 *C*). Hence, these results show that the presence of the UCS domain alone is sufficient to prevent misfolding of the myosin motor domain.

In the second method, we examined the thermal aggregation of S1 in the presence of full-length UNC-45B, UCS or Central domain. The time-dependent aggregation of myosin S1 in the presence of BSA (control) at 43°C is shown in Fig. 4 *D* (*solid squares*). In the presence of 1 $\mu$M UNC-45B (*open triangles*) or 1 $\mu$M UCS (*solid circles*) aggregation was reduced by >90%. In contrast, we found that the Central domain does not protect against S1 aggregation. These results are in agreement with the AFM experiments and indicate that the UCS domain alone is sufficient to prevent aggregation of myosin motor domain, and that the Central domain does not possess these features.

## CONCLUSIONS

UNC-45B has a unique architecture for a molecular chaperone. It contains three domains with distinct functions: the N-terminal TPR domain that binds and recruits Hsp90, the Central domain that independently binds the myosin head (Fig. 3), and the C-terminal UCS domain that independently interacts with the myosin head (Fig. 3) and prevents thermal aggregation and maintains mechanically unfolded

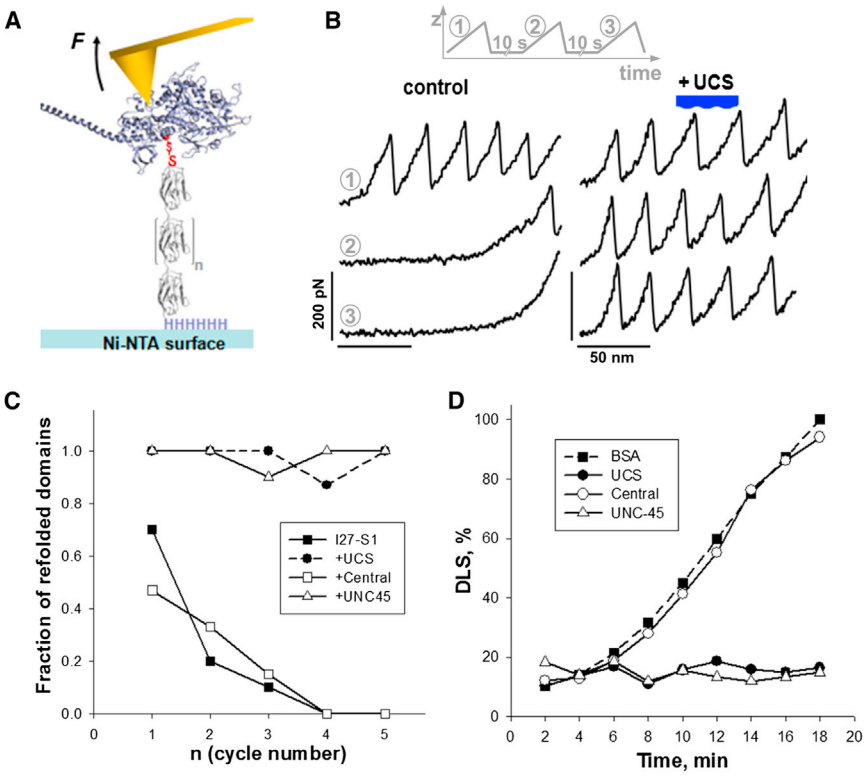


FIGURE 4 The UCS but not the Central domain is sufficient to prevent misfolding and aggregation of the myosin motor domain. (*A*) The myosin motor domain (*purple*) was derivatized with a mechanical reporter, a tandem repeat I27 polyprotein (*gray*) carrying an N-terminal cysteine residue, and a C-terminal $His_6$ tag. The I27 polyprotein serves both a handle attached to the reactive cysteines in S1 and a reporter of force-driven unfolding and refolding reactions. The handle introduces a means of site-specific attachment via the $His_6$ tag. (*B*) Single I27−S1 molecules were repeatedly unfolded and refolded. Misfolding of the I27-S1 chimera is observed in the absence of the chaperone (control), whereas full recovery is observed in the presence of 1 $\mu$M UCS domain (*right panel*). (*C*) Plot of the fraction of refolded I27 domains as a function of the refolding cycles. Single- I27−S1 molecules in the absence of chaperone (*solid squares*), + 1 $\mu$M Central (*open squares*), + 1 $\mu$M full-length UNC-45B (*triangles*) or + 1 $\mu$M UCS (*solid circles*) were subjected to repeated cycles of unfolding/refolding. (*D*) Thermal aggregation of the myosin S1 (1 $\mu$M) at 43°C measured by dynamic light scattering (532 nm) in the presence of BSA (*squares*), UCS (*solid circles*), Central domain (*open circles*), and full-length UNC-45 (*triangles*), all at 1 $\mu$M. To see this figure in color, go online.

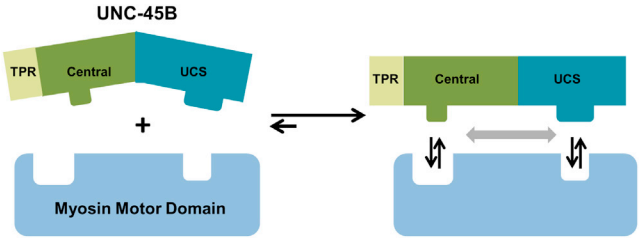


FIGURE 5 Hypothetical model for UNC-45B−Myosin motor domain complex formation. We propose that each UNC-45B domain engages different binding subsites on the myosin client protein. To see this figure in color, go online.

intermediates of the myosin head competent for refolding (Fig. 4).

Our experiments indicate that the UNC-45B−myosin head binding site is built of two binding subsites, each engaging a different UNC-45B domain. The domains display different interaction energetics; the affinity of myosin for UCS domain is higher (~$4.3 \times 10^6$ $M^{-1}$) than for the Central domain (~$6 \times 10^5$ $M^{-1}$). Interestingly, the affinity of myosin for the UCS domain is higher than for full-length UNC-45B (~$2.8 \times 10^6$ $M^{-1}$). We propose a model in which different domains of UNC-45B bind to distinct subsites on the myosin motor domain with different functional consequences (Fig. 5). While both the UCS and the Central domain bind the myosin head with high affinity, only the UCS domain displays chaperone activity. Our data suggest that the formation of the UNC-45B−motor domain complex is accompanied by allosteric and conformational transitions. We calculated a free energy change accompanying the allosteric conformational transitions of ~−8 kcal/mol. The significant energetic penalty of the simultaneous engagement of the two UNC-45B domains with the myosin head indicates that the domains are not thermodynamically autonomous and that allosteric interactions may play a role in modulating the chaperone-myosin interactions. Although our results indicate that the Central domain might be involved in the formation of the UNC-45B–myosin complex, its exact function still remains unclear and may be related to the dynamics of the chaperone release from the myosin. Our laboratory is currently examining these processes.

## SUPPORTING MATERIAL

Materials and Methods, two figures, and 16 equations are available at http://www.biophysj.org/biophysj/supplemental/S0006-3495(14)00630-4.

We greatly thank Professor Wlodek Bujalowski for stimulating discussions, for helpful comments, and for a critical reading of the manuscript.

This work was funded by American Heart Association grant No. 13GRNT17290006, National Institutes of Health/National Institute on Aging grant No. P30AG024832, the John Sealy Memorial Endowment Fund for Biomedical Research, and the Cecil M. Green Endowment at the University of Texas Medical Branch.

## REFERENCES

1. Bartlett, A. I., and S. E. Radford. 2009. An expanding arsenal of experimental methods yields an explosion of insights into protein folding mechanisms. *Nat. Struct. Mol. Biol.* 16:582–588.
2. Hartl, F. U. 1996. Molecular chaperones in cellular protein folding. *Nature.* 381:571–579.
3. Tang, Y. C., H. C. Chang, …, M. Hayer-Hartl. 2006. Structural features of the GroEL-GroES nano-cage required for rapid folding of encapsulated protein. *Cell.* 125:903–914.
4. Chakraborty, K., M. Chatila, …, M. Hayer-Hartl. 2010. Chaperonin-catalyzed rescue of kinetically trapped states in protein folding. *Cell.* 142:112–122.
5. Brinker, A., G. Pfeifer, …, M. Hayer-Hartl. 2001. Dual function of protein confinement in chaperonin-assisted protein folding. *Cell.* 107:223–233.
6. Hartl, F. U., A. Bracher, and M. Hayer-Hartl. 2011. Molecular chaperones in protein folding and proteostasis. *Nature.* 475:324–332.
7. Gaiser, A. M., C. J. Kaiser, …, K. Richter. 2011. Downregulation of the Hsp90 system causes defects in muscle cells of *Caenorhabditis elegans*. *PLoS ONE.* 6:e25485.
8. Hawkins, T. A., A. P. Haramis, …, S. W. Wilson. 2008. The ATPase-dependent chaperoning activity of Hsp90a regulates thick filament formation and integration during skeletal muscle myofibrillogenesis. *Development.* 135:1147–1156.
9. Gazda, L., W. Pokrzywa, …, T. Clausen. 2013. The myosin chaperone UNC-45 is organized in tandem modules to support myofilament formation in *C. elegans*. *Cell.* 152:183–195.
10. Barral, J. M., A. H. Hutagalung, …, H. F. Epstein. 2002. Role of the myosin assembly protein UNC-45 as a molecular chaperone for myosin. *Science.* 295:669–671.
11. Kachur, T. M., and D. B. Pilgrim. 2008. Myosin assembly, maintenance and degradation in muscle: role of the chaperone UNC-45 in myosin thick filament dynamics. *Int. J. Mol. Sci.* 9:1863–1875.
12. Srikakulam, R., and D. A. Winkelmann. 2004. Chaperone-mediated folding and assembly of myosin in striated muscle. *J. Cell Sci.* 117:641–652.
13. Lord, M., and T. D. Pollard. 2004. UCS protein Rng3p activates actin filament gliding by fission yeast myosin-II. *J. Cell Biol.* 167:315–325.
14. Yu, Q., and S. I. Bernstein. 2003. UCS proteins: managing the myosin motor. *Curr. Biol.* 13:R525–R527.
15. Etard, C., M. Behra, …, U. Strähle. 2007. The UCS factor Steif/Unc-45b interacts with the heat shock protein Hsp90a during myofibrillogenesis. *Dev. Biol.* 308:133–143.
16. Foth, B. J., M. C. Goedecke, and D. Soldati. 2006. New insights into myosin evolution and classification. *Proc. Natl. Acad. Sci. USA.* 103:3681–3686.
17. Sellers, J. R. 2000. Myosins: a diverse superfamily. *Biochim. Biophys. Acta.* 1496:3–22.
18. Srikakulam, R., and D. A. Winkelmann. 1999. Myosin II folding is mediated by a molecular chaperonin. *J. Biol. Chem.* 274:27265–27273.
19. Chow, D., R. Srikakulam, …, D. A. Winkelmann. 2002. Folding of the striated muscle myosin motor domain. *J. Biol. Chem.* 277:36799–36807.
20. Barral, J. M., C. C. Bauer, …, H. F. Epstein. 1998. Unc-45 mutations in *Caenorhabditis elegans* implicate a CRO1/She4p-like domain in myosin assembly. *J. Cell Biol.* 143:1215–1225.
21. Hellerschmied, D., and T. Clausen. 2014. Myosin chaperones. *Curr. Opin. Struct. Biol.* 25C:9–15.
22. Landsverk, M. L., S. Li, …, H. F. Epstein. 2007. The UNC-45 chaperone mediates sarcomere assembly through myosin degradation in *Caenorhabditis elegans*. *J. Cell Biol.* 177:205–210.
23. Price, M. G., M. L. Landsverk, …, H. F. Epstein. 2002. Two mammalian UNC-45 isoforms are related to distinct cytoskeletal and muscle-specific functions. *J. Cell Sci.* 115:4013–4023.

24. Ni, W., A. H. Hutagalung, …, H. F. Epstein. 2011. The myosin-binding UCS domain but not the Hsp90-binding TPR domain of the UNC-45 chaperone is essential for function in *Caenorhabditis elegans*. *J. Cell Sci.* 124:3164–3173.

25. Melkani, G. C., C. F. Lee, …, S. I. Bernstein. 2010. *Drosophila* UNC-45 prevents heat-induced aggregation of skeletal muscle myosin and facilitates refolding of citrate synthase. *Biochem. Biophys. Res. Commun.* 396:317–322.

26. Kaiser, C. M., P. J. Bujalowski, …, A. F. Oberhauser. 2012. Tracking UNC-45 chaperone-myosin interaction with a titin mechanical reporter. *Biophys. J.* 102:2212–2219.

27. Shi, H., and G. Blobel. 2010. UNC-45/CRO1/She4p (UCS) protein forms elongated dimer and joins two myosin heads near their actin binding region. *Proc. Natl. Acad. Sci. USA.* 107:21382–21387.

28. Lee, C. F., A. V. Hauenstein, …, T. Huxford. 2011. X-ray crystal structure of the UCS domain-containing UNC-45 myosin chaperone from *Drosophila melanogaster*. *Structure.* 19:397–408.

29. Pollard, T. D. 1982. Myosin purification and characterization. *Methods Cell Biol.* 24:333–371.

30. Weeds, A. G., and B. Pope. 1977. Studies on the chymotryptic digestion of myosin. Effects of divalent cations on proteolytic susceptibility. *J. Mol. Biol.* 111:129–157.

31. Mornet, D., K. Ue, and M. F. Morales. 1984. Proteolysis and the domain organization of myosin subfragment 1. *Proc. Natl. Acad. Sci. USA.* 81:736–739.

32. Bullard, B., W. A. Linke, and K. Leonard. 2002. Varieties of elastic protein in invertebrate muscles. *J. Muscle Res. Cell Motil.* 23:435–447.

33. Carrion-Vazquez, M., A. F. Oberhauser, …, J. M. Fernandez. 1999. Mechanical and chemical unfolding of a single protein: a comparison. *Proc. Natl. Acad. Sci. USA.* 96:3694–3699.

34. Miller, E., T. Garcia, …, A. F. Oberhauser. 2006. The mechanical properties of *E. coli* type 1 pili measured by atomic force microscopy techniques. *Biophys. J.* 91:3848–3856.

35. Oberhauser, A. F., C. Badilla-Fernandez, …, J. M. Fernandez. 2002. The mechanical hierarchies of fibronectin observed with single-molecule AFM. *J. Mol. Biol.* 319:433–447.

36. Oberhauser, A. F., P. E. Marszalek, …, J. M. Fernandez. 1998. The molecular elasticity of the extracellular matrix protein tenascin. *Nature.* 393:181–185.

37. Florin, E. L., M. Rief, …, H. E. Gaub. 1995. Sensing specific molecular interactions with the atomic force microscope. *Biosens. Bioelectron.* 10:895–901.

38. Sakaki, N., R. Shimo-Kon, …, K. Kinosita, Jr. 2005. One rotary mechanism for F1-ATPase over ATP concentrations from millimolar down to nanomolar. *Biophys. J.* 88:2047–2056.

39. Rief, M., M. Gautel, …, H. E. Gaub. 1997. Reversible unfolding of individual titin immunoglobulin domains by AFM. *Science.* 276:1109–1112.

40. Reference deleted in proof.

41. Reference deleted in proof.

42. Reference deleted in proof.

43. Reference deleted in proof.

44. Hiratsuka, T. 1999. ATP-induced opposite changes in the local environments around $Cys^{697}$ (SH2) and $Cys^{707}$ (SH1) of the myosin motor domain revealed by the prodan fluorescence. *J. Biol. Chem.* 274:29156–29163.

45. Lakowicz, J. R. 2006. Principles of Fluorescence Spectroscopy. Springer Science+Business Media, Boston, MA.

46. Bujalowski, W., and T. M. Lohman. 1987. A general method of analysis of ligand-macromolecule equilibria using a spectroscopic signal from the ligand to monitor binding. Application to *Escherichia coli* single-strand binding protein-nucleic acid interactions. *Biochemistry.* 26:3099–3106.

47. Bujalowski, W. 2006. Thermodynamic and kinetic methods of analyses of protein-nucleic acid interactions. From simpler to more complex systems. *Chem. Rev.* 106:556–606.

48. Bujalowski, W., and M. J. Jezewska. 2011. Macromolecular competition titration method accessing thermodynamics of the unmodified macromolecule-ligand interactions through spectroscopic titrations of fluorescent analogs. *Methods Enzymol.* 488:17–57.

49. Jencks, W. P. 1981. On the attribution and additivity of binding energies. *Proc. Natl. Acad. Sci. USA.* 78:4046–4050.

50. Oberhauser, A. F., and M. Carrión-Vázquez. 2008. Mechanical biochemistry of proteins one molecule at a time. *J. Biol. Chem.* 283:6617–6621.